Science of the Total Environment 603–604 (2017) 308–318

Contents lists available at ScienceDirect

Science of the Total Environment

journal homepage: www.elsevier.com/locate/scitotenv

Spatial distribution of trace element Ca-normalized ratios in primary and permanent human tooth enamel

Théo Tacail [a], Lenka Kovačiková [b], Jaroslav Brůžek [c], Vincent Balter [a,*]

[a] Laboratoire de Géologie de Lyon, UMR 5276 CNRS, Ecole Normale Supérieure de Lyon, 46, Allée d'Italie, 69364 Lyon Cedex 07, France
[b] Laboratory of Archaeobotany and Palaeoecology, Faculty of Science, University of South Bohemia, Na Zlaté stoce 3, 370 05 České Budějovice, Czech Republic
[c] Department of Anthropology and Human Genetics, Faculty of Sciences, Charles University, Viničná 7, 128 43 Prague, Czech Republic

HIGHLIGHTS

- A comprehensive framework of the distribution of some trace elements in tooth enamel is proposed.
- Ca-normalized ratios of Cu, Ni, Zn, Sr and Ba discriminate deciduous \and permanent teeth.
- It is recommended to perform laser ablation rasters along the dentine-enamel junction.
- The transfer of these elements to human enamel is discussed.

GRAPHICAL ABSTRACT

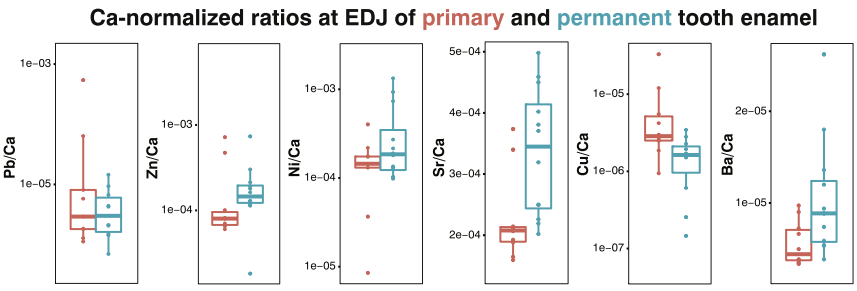

ARTICLE INFO

Article history:
Received 22 March 2017
Received in revised form 1 June 2017
Accepted 3 June 2017
Available online xxxx

Editor: D. Barcelo

Keywords:
Tooth enamel
Laser ablation
Strontium
Barium
Transition metals

ABSTRACT

The trace elements distribution embedded in tooth enamel offers a means to study exposure of toxic metals and allows the reconstruction of dietary behaviors. The quantification of most of the elements with a spatial high resolution (~50 μm) is routinely achieved using laser ablation inductively coupled plasma mass spectrometry (LA-ICPMS). However, the lack of a comprehensive framework of trace elements distribution in enamel jeopardizes any endorsed sampling strategy using LA-ICPMS. The present work is an effort to improve our knowledge on this issue. We studied a suite of 22 sectioned teeth with known dietary history, including 12 3rd molars from 12 living individuals and 10 primary teeth from 3 living individuals. Using LA-ICPMS, we measured Ca, Cu, Zn, Ni, Sr, Ba and Pb variations along 2 or 3 rasters from cervical to occlusal enamel. Calcium concentrations are lower in primary than in permanent teeth and do not vary spatially within a tooth suggesting that enamel matures homogeneously before eruption. The Pb/Ca ratio does not vary within tooth enamel and between primary and permanent tooth enamel. The Cu/Ca and Ni/Ca ratios do not vary within tooth enamel but discriminate primary from permanent tooth enamel. The Zn/Ca ratios are higher in permanent than in primary tooth enamel, and increase up to an order of magnitude in the last hundred of microns at the enamel surface. The Sr/Ca and Ba/Ca ratios are higher in permanent than in primary tooth enamel, and decrease from the enamel-dentine junction towards outer enamel in permanent but not in primary tooth enamel. Considering the Ca-normalized intra-tooth variations of Zn, Sr and Ba, we recommend to perform laser ablation rasters along the enamel-dentine junction because this area is likely to retain most of the original and complete chemical information related to individual's life.

* Corresponding author.
E-mail address: Vincent.Balter@ens-lyon.fr (V. Balter).

http://dx.doi.org/10.1016/j.scitotenv.2017.06.021
0048-9697/

1. Introduction

The trace elements distribution embedded in tooth enamel represents an archive of the environmental conditions that prevailed when the tooth was forming, but this information needs to be deciphered using appropriate techniques. Since the first study published around 1995 (Cox et al., 1996; Evans et al., 1995), laser ablation hyphenated to inductively coupled plasma mass spectrometer (LA-ICPMS) is becoming increasingly utilized for analyzing tooth enamel in toxicological and archaeological sciences. Two main reasons explain this keen interest. The first is linked to the ICPMS capabilities, such as large linear response, low limits of detection (<μg/g) and multi-elemental analysis (e.g. Pozebon et al., 2014). The second reason is that enamel has an incremental structure that allows the spatial reconstruction of chemical variations in relation to growth patterns (e.g. Outridge et al., 1995). Three main avenues of research are currently analyzing teeth with LA-ICPMS: toxicology, paleobiology and diagenesis. Exposure of toxic metals, such as Pb, and further incorporation in the body can be monitored by analyzing tooth enamel levels and spatial distribution (Arora et al., 2006, 2011; Asaduzzaman et al., 2017; Budd et al., 1998; Evans et al., 1995; Farell et al., 2013; Hanć et al., 2013; Hare et al., 2011, Hoffmann et al., 2000; Lee et al., 1999; Modabbernia et al., 2016; Shepherd et al., 2012, 2016). Ingestion of metals that are segregated by mammal metabolism, such as Sr and Ba, and whose dietary level dramatically change during weaning, can be reconstructed by analyzing spatial variations in tooth enamel (Austin et al., 2013; Balter et al., 2012; Dolphin et al., 2005; Guede et al., 2017; Humphrey et al., 2008; Kang et al., 2004; Kohn et al., 2013; Lochner et al., 1999; Lugli and Cipriani, 2017; Vašinová Galiová et al., 2013). Regarding archaeological applications, the effects of post-mortem incorporation of elements in fossil teeth can also be scrutinized by LA-ICPMS (Balter et al., 2012; Cox et al., 1996; Cucina et al., 2007; Kohn et al., 2013; Hinz and Kohn, 2010; Eggins et al., 2003; Grün et al., 2009; Kohn and Moses, 2013; Reynard and Balter, 2014).

A concern for studying the chemical composition of tooth enamel by means of LA-ICPMS is to decipher chemical variations linked to age-related changes from those generated by enamel formation and dental growth. Amelogenesis (tooth enamel formation) occurs through two subsequent steps, the matrix deposition step and the enamel maturation step (Suga, 1982). An organic-rich and poorly crystallized matrix is first produced by ameloblasts during the maturation step. The matrix further matures, i.e. crystallizes, under the influence of mineralization waves (Suga, 1982) that sweep dental crown in various directions. The enamel maturation step is thus a three-dimensional process which anisotropically damps the primary signal recorded during the matrix deposition step. The crystallization of enamel occurs at the expense of chemical impurities, such as carbonate (CO_3) and magnesium (Mg) which are partially removed during the process (Aoba, 1996; Aoba and Moreno, 1990, 1992; Lundgren et al., 1998). Humphrey et al. (2008) also document a systematic decrease of the strontium/calcium (Sr/Ca) ratio from the enamel-dentine junction (EDJ) towards outer enamel, consistent with the degree of mineral density observed in dental enamel, using X-ray microradiography (Wilson and Beynon, 1989; Wong et al., 2004). Zazzo et al. (2005) also document that outer enamel is much more crystallized than inner enamel on the basis of a systematic decrease of the CO_3 content from EDJ to outer enamel.

Independently of the deposition-maturation processes that lead to three-dimensional mixing in enamel, the crescent-shaped geometry of the enamel crown is a source of spatial heterogeneities. Enamel close to the occlusal surface, or occlusal enamel, is thicker than that close to the cervix, i.e. cervical enamel. While cervical enamel forms after occlusal enamel, and thus will not document the same period of time exactly, it will also record a more condensed history than occlusal enamel due to its lower thickness. Because different parts of the enamel crown will not record the same history due to asynchronous formation and varied maturation local intensities, the measurement strategy is a crucial issue.

Ideally, teeth must be sectioned to have a flat surface suitable for the laser ablation technique. It is in some cases however impossible, like for precious fossil samples such as hominins teeth. The laser ablation is thus performed on the surface of the enamel but this can lead to instrumental elemental and isotopic fractionation (Jackson and Günther, 2003) because the laser can be unfocused if the surface is too curved. Working with laser ablation on the surface of a tooth can yield accurate but locally restricted results (Le Roux et al., 2014), which can be problematic for highly variable parameter such as the $^{87}Sr/^{86}Sr$ ratio (Copeland et al., 2011; Balter et al., 2012). An alternative is to work on broken teeth and perform the ablation profiles along the crack (Cucina et al., 2007; Balter et al., 2012). So far however, almost all of the studies have been conducted on enamel of sectioned teeth. For the oldest studies, labs were not equipped with automatic sample holder and the ablation mode was using laser spots (Cox et al., 1996; Evans et al., 1995). Further studies were focused on the differences between enamel and dentine, being biogenic or diagenetic, and laser rasters were performed along longitudinal sections covering dentine and enamel (Eggins et al., 2003; Kohn et al., 2013; Lee et al., 1999; Budd et al., 2000). Other studies used rasters parallel to the EDJ on both sides of the neonatal line (Kang et al., 2004; Lochner et al., 1999; Dolphin et al., 2005; Arora et al., 2006). Nowadays, it is possible to obtain, thanks to big data computing, a full bioimage of concentrations (Arora et al., 2011; Austin et al., 2013; Grün et al., 2009; Hare et al., 2011; Hinz and Kohn, 2010; Humphrey et al., 2008; Vašinová Galiová et al., 2013). The results are usually impressive, but the technique is still highly time consuming (and a as consequence expensive), even if the bioimage is interpolated from a grid of spots.

In conclusion, there is still a need for a fast and reliable strategy to analyze tooth enamel by means of LA-ICPMS. In the present work, we have analyzed calcium (Ca), copper (Cu), zinc (Zn), nickel (Ni), strontium (Sr), barium (Ba) and lead (Pb) in a suite of 22 sectioned teeth, for which 2 or 3 rasters were performed from cervix enamel to apex enamel. We propose that the most suitable location to perform laser ablation profile is along the EDJ, because this area retains most of the information without significant attenuation.

2. Material

2.1. Samples and ethical considerations

The material is composed of twelve third molars from twelve individuals and ten primary teeth from three individuals (Table 1). Third

Table 1
Description of the samples used in the present study.

Sample id		Tooth	FDI	Sex	Birth	Menarche (y.o.)
Permanent teeth						
1	AB-M3	3rd molar sup right	48	F	1958	–
2	AJT-M3	3rd molar sup left	38	F	1948	11
3	CMJ-M3	3rd molar sup right	48	F	1948	12
4	DA-M3	3rd molar sup right	48	M	1962	NA
5	EP-M3	3rd molar sup left	38	F	1983	12
6	LW-M3	3rd molar sup left	38	F		10
7	MG-M3	3rd molar sup left	38	M	1985	NA
8	MV-M3	3rd molar sup left	38	F	1948	–
9	OO-M3	3rd molar sup right	48	M	1964	NA
10	SL-M3	3rd molar sup right	48	M	1985	NA
11	WI-M3	3rd molar sup right	48	M	1948	NA
12	ZA-M3	3rd molar sup left	38	F	1981	12
Primary teeth						
13	DB-c	Canine sup right	53	F	1947	NA
14	DB-i1	1st incisor inf	71/81	F	1947	NA
15	DB-i2	2nd incisor inf	72/82	F	1947	NA
16	PB-c	Canine sup right	53	M	1973	NA
17	PB-i	1st incisor inf	71/81	M	1973	NA
18	PB-m1	1st molar sup right	16	M	1973	NA
19	PB-m2	2nd molar sup right	17	M	1973	NA
20	VB-i2	2nd incisor sup left	62	M	1971	NA
21	VB-m1	1st molar sup right	54	M	1971	NA
22	VB-m2	2nd molar inf right	85	M	1971	NA

Table 2
Optimized settings of the ICPMS (Thermo XSeries) and Excite 193 nm ArF Excimer laser system (Photon Machines, MT, USA).

Excite 193 nm LA system (Photon Machine)	
Cell type	Helex chamber
LA pulse width	<4 ns
He carrier MFC1 flow [L min^{-1}]	0.9
He carrier MFC2 flow [L min^{-1}]	0.4
Maximal fluence [J cm^{-1}]	15.2
Delivered fl. [% of max. fl.]	70–100
Raster scan lengths [μm]	500–600
Scan speed [μm s^{-1}]	10
Spot size (diameter) [μm]	85
Repetition rate [Hz]	15
Washout time [s]	30
ICPMS (Thermo ×7 series)	
RF-power [W]	1350
Gaz-flows	
Sample Ar [L min^{-1}]	1
Coolant Ar [L min^{-1}]	13
Auxiliary Ar [L min^{-1}]	0.8

molars were removed for surgical reasons and primary teeth were naturally shed. Each tooth was first sectioned longitudinally along bucco-lingual axis using a diamond saw. A resulting half-tooth was embedded in araldite resin, and the cut face polished with waterproof silicon carbide paper with a grid up to 4000 to obtain a plane surface.

All teeth were naturally shed or extracted for surgical purposes in accordance with the World Medical Association's Declaration of Helsinki. In each case, the informed consent of the patients or their parents was collected. Some of the teeth were already used to measure Ca (Tacail et al., 2017), Cu and Fe (Jaouen et al., 2017) isotope compositions.

2.2. Standards

One analytical difficulty using LA-ICPMS is the calibration step, i.e. the determination of a transfer function that correlates the signal of a given mass to real concentration. An accurate calibration must take into account elemental fractionation that occur during sample vaporization by the laser, transport to the ICPMS, atomization and ionization in the plasma (Miliszkiewicz et al., 2015). Because the signal is matrix dependent, the calibration must involve the use of sample matrix-matched standards. Tooth tissues, being enamel or dentine, are composed of carbonate hydroxylapatite (CHA), a calcium phosphate ($Ca_{10}(PO_4)_6(OH)_2$, Legeros and Legeros, 1984). In tooth enamel, CHA is well crystallized and organic matter is almost absent (primary enamel ~0.7%, permanent enamel ~0.6%, Stack, 1955), while in dentine, CHA is less crystallized and the amount of organic matter (collagen) can reach 20% (Stack, 1955). Here, the calibration procedure was performed using sintered international standard SRM1400 and in-house precipitated CHA (HAPp1). The precipitation of HAPp1 was performed according to the procedure of Balter and Lécuyer (2004) and details are given in Tacail et al. (2016). The sintering procedure was performed using Spark Plasma Sintering (SPS) technique. All the technical details regarding the sintering procedure are given in Tacail et al. (2016).

3. Method

3.1. Laser ablation

Analyses in the LA mode were carried out using an Excite 193 nm ArF Excimer laser system (Photon Machines, MT, USA). The mounted HeLex cell allowed ablation of samples in an ultrapure He atmosphere with efficient recovery of the ablated material. All the technical details are developed in Tacail et al. (2015) and the operating settings given in Table 2.

3.2. ICPMS

A quadrupole ICPMS (Thermo XSeries) was used for the measurement of trace elements concentrations. Operating settings are given in Table 2. Selected monitored isotopes were ^{46}Ca, ^{62}Ni, ^{63}Cu, ^{66}Zn, ^{68}Zn, ^{86}Sr, ^{88}Sr, ^{137}Ba, ^{138}Ba and ^{207}Pb. Two isotopes were measured for Ca, Zn, Sr and Ba to check the accuracy of the concentrations irrespectively of the selected isotope and similar results were obtained in all cases. No major interference were noticed on these masses. It is difficult to calculate the limit of detection of the method because it depends heavily on the laser ablation settings. However, a rough evaluation of the signal/blank ratio for the SRM1400 international standard gives a value between 5 and 10 for ^{62}Ni (~6 μg/g in SRM1400), ^{63}Cu (~2 μg/g), ^{66}Zn (~180 μg/g), ^{68}Zn and ^{207}Pb (~9 μg/g), and higher than 10^3 for ^{86}Sr (~250 μg/g), ^{88}Sr, ^{137}Ba (~250 μg/g) and ^{138}Ba. The mass 46 was preferred over 43 for Ca, because the ^{43}Ca signal was sometimes too high and likely to generate a non-linear response of the detector, and also because the signal/blank ratio was better for ^{46}Ca than for ^{43}Ca. All the analysis were performed over one week and, as the settings for the laser ablation and the ICPMS were found to be very stable, they were kept unchanged during the whole session.

3.3. Sequence procedure

We initially performed LA analysis by calibrating the samples with the SRM1400 standard, but we noticed that the Sr/Ca ratio, but more importantly the Ba/Ca ratio, of the samples were much lower than those of the SRM1400 (Table 3). We thus performed the calibration of the samples by using the standard HAPp1 in order to have a better match between the samples and the standards in terms of concentration. A typical sequence was structured as following: blank, HAPp1, sample 1, HAPp1, sample 2, HAPp1, sample 3, HAPp1. Blanks values were obtained by acquiring data on the mass spectrometer during fifty seconds without firing the laser. In general, three LA profiles were performed on a single tooth, except for some of the primary teeth for which two LA profiles only were performed. All the LA profiles started from the extremity of the cervix enamel bevel and ran towards the apex enamel. The LA profiles were labeled "EDJ", "MID" and "OUT" to describe their position within the enamel crown.

3.4. Data processing

The LA-ICPMS technique generates a great amount of data that need to be treated and reduced to be interpreted accurately. For instance, in

Table 3
Comparison of the values of the Ca-normalized Ni, Zn, Cu, Sr and Ba ratios of the HAPp1 in-house standard measured in the present study using laser ablation with the values obtained in the solution mode, and of the international standard SRM1400 measured in the present study using laser ablation with the certified values published in Hinners et al. (1998).

	Ni/Ca	Zn/Ca	Cu/Ca	Sr/Ca	Ba/Ca	Pb/Ca
Average ratio in the present study	$\sim 3 \times 10^{-4}$	$\sim 7 \times 10^{-4}$	$\sim 2 \times 10^{-7}$	$\sim 3 \times 10^{-4}$	$\sim 8 \times 10^{-6}$	$\sim 3 \times 10^{-5}$
HAPp1 measured in Lyon	1.7×10^{-4}	7.8×10^{-6}	2.1×10^{-6}	2.0×10^{-4}	3.4×10^{-6}	1.0×10^{-6}
SRM1400 measured in Lyon	3.9×10^{-5}	4.5×10^{-4}	9.2×10^{-6}	6.5×10^{-4}	6.6×10^{-4}	2.3×10^{-5}
SRM1400 certified value (Hinners et al., 1998)	1.5×10^{-5}	4.7×10^{-4}	6.1×10^{-6}	6.5×10^{-4}	6.3×10^{-4}	2.3×10^{-5}

Table 4
Description of the different steps of data processing.

Step	Description
#1	Splitting of blank values for each isotope
#2	Calculation of average blank values for each isotope
#3	Blank values substraction for each isotope
#4	Splitting of the plateau on the ^{46}Ca isotope basis
#5	Applying the limits of the ^{46}Ca plateau on each isotope
#6	Calculating elemental signals from isotopic signal
#7	Normalization of each element to Ca
#8	3 sigma filter for each x/Ca ratio on each standard
#9	Calculation of average x/Ca ratio for each standard
#10	Sample-standard bracketing for each x/Ca ratio
#11	2.5 sigma local filter for each x/Ca ratio on each sample
#12	Moving-average for each x/Ca ratio on each sample
#13	Statistics for each x/Ca ratio on each sample

the present study, we generated a 11 × 132,000 matrix after 4 days of work only. We thus developed a numerical procedure using the Python programming language. All the steps are given in Table 4.

4. Results

Reduced data are given for each profile in Supplementary Table 1 and all the profiles with x/Ca ratio variations are given in the Supplementary Information Profiles. Except in few cases for the Ni/Ca, Cu/Ca and Pb/Ca ratios, elemental concentrations in dental enamel were high enough to produce profiles with reliable variations.

Calcium concentrations, which are given by HAPp1-normalized ^{46}Ca counts per second (cps), are significantly lower ($P = 0.0259$) in primary ($cps = 9.52 \times 10^8 \pm 1.22 \times 10^8$) than in permanent tooth enamel ($cps = 1.05 \times 10^9 \pm 2.05 \times 10^8$). This is consistent with the observation of Wilson and Beynon (1989) using quantitative microradiography, that mineralization levels are lower in the primary dentition. Calcium concentrations do not vary spatially from the inner part of the tooth enamel close to the EDJ towards outer enamel, suggesting that enamel matures homogeneously before eruption, both in permanent (Fig. 1A) and primary (Fig. 1B) teeth.

For the Pb/Ca ratios, we do not observe any significant variations between primary and permanent tooth enamel ($P = 0.2103$, Fig. 2A) and within tooth enamel (Figs. 3A and 4A). This is probably due to the very low level of Pb in recent enamel (below the μg/g level). Some profiles exhibit noticeably high average Pb, notably DB-c-out and in a lesser extent EP-M3-out or MG-M3-out (Supplementary Information Profiles). The DB-c-out profile has been obtained on a primary tooth and is due the presence of local and very concentrated Pb spikes, probably generated through the consumption of Pb-contaminated drinking water. The EP-M3-out and MG-M3-out profiles come from permanent teeth for which the Pb contamination has been less acute (Asaduzzaman et al., 2017).

The Ni/Ca ratios are higher in permanent teeth than in primary teeth ($P = 0.0049$, Fig. 2B), but do not vary within tooth enamel (Figs. 3B and 4B). Inversely, the Cu/Ca ratios are higher in primary teeth than in permanent teeth ($P = 0.0273$, Fig. 2C), and as the Ni/Ca ratios, do not vary within tooth enamel (Figs. 3C and 4C).

When the "EDJ", "MID" and "OUT" profiles are considered altogether, the Zn/Ca ratios are similar in permanent and in primary tooth enamel ($P = 0.2913$, Fig. 2D). However, this bulk approach does not integrate the highly heterogeneous Zn distribution in tooth enamel. The Zn/Ca ratio increases to up an order of magnitude in the last hundred of microns at the enamel surface in both primary (Fig. 3D) and permanent (Fig. 4D) teeth.

The Sr/Ca and Ba/Ca ratios are higher in permanent than in primary tooth enamel (Sr, $P = 0.0014$, Fig. 2E; Ba, $P = 0.0046$, Fig. 2F), and decrease from the EDJ towards outer enamel in permanent (Sr/Ca, Fig. 3E; Ba/Ca, Fig. 3F) but not in primary (Sr/Ca, Fig. 4E; Ba/Ca, Fig. 4F) tooth enamel. For the Sr/Ca ratio, these observations are in accordance with the results of Humphrey et al. (2008), Balter et al. (2008, 2012), but this is the first demonstration that the Ba/Ca ratio also decrease from the EDJ towards outer enamel.

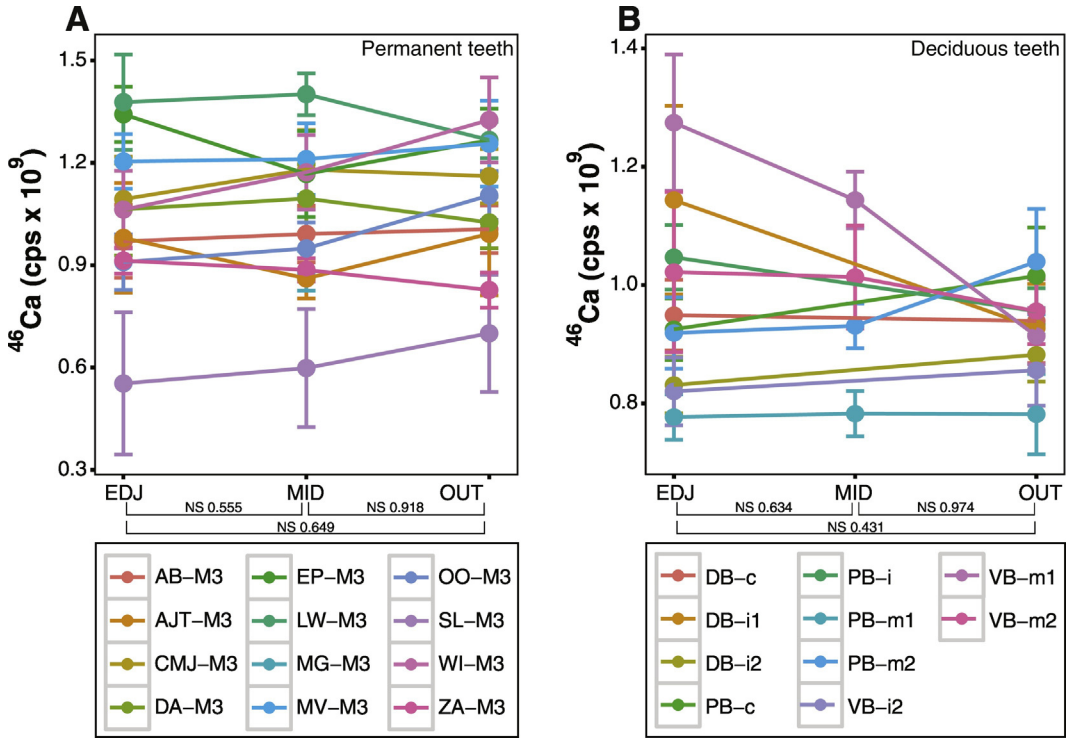

Fig. 1. Distribution of the ^{46}Ca concentration, given by ^{46}Ca counts per second for the EDJ, MID and OUT profiles in permanent teeth (A) and primary teeth (B). The ^{46}Ca signal of the samples is corrected by that of the HAPp1 standard. Statistical difference between groups of profiles is estimated using two-tailed Student's *t*-tests *P* values (*P*). For all panels, NS $P > 0.05$, $^*P = 0.01$–0.05, $^{**}P = 0.001$–0.01, and $^{***}P < 0.001$. (For interpretation of the references to colour in this figure legend, the reader is referred to the web version of this article.)

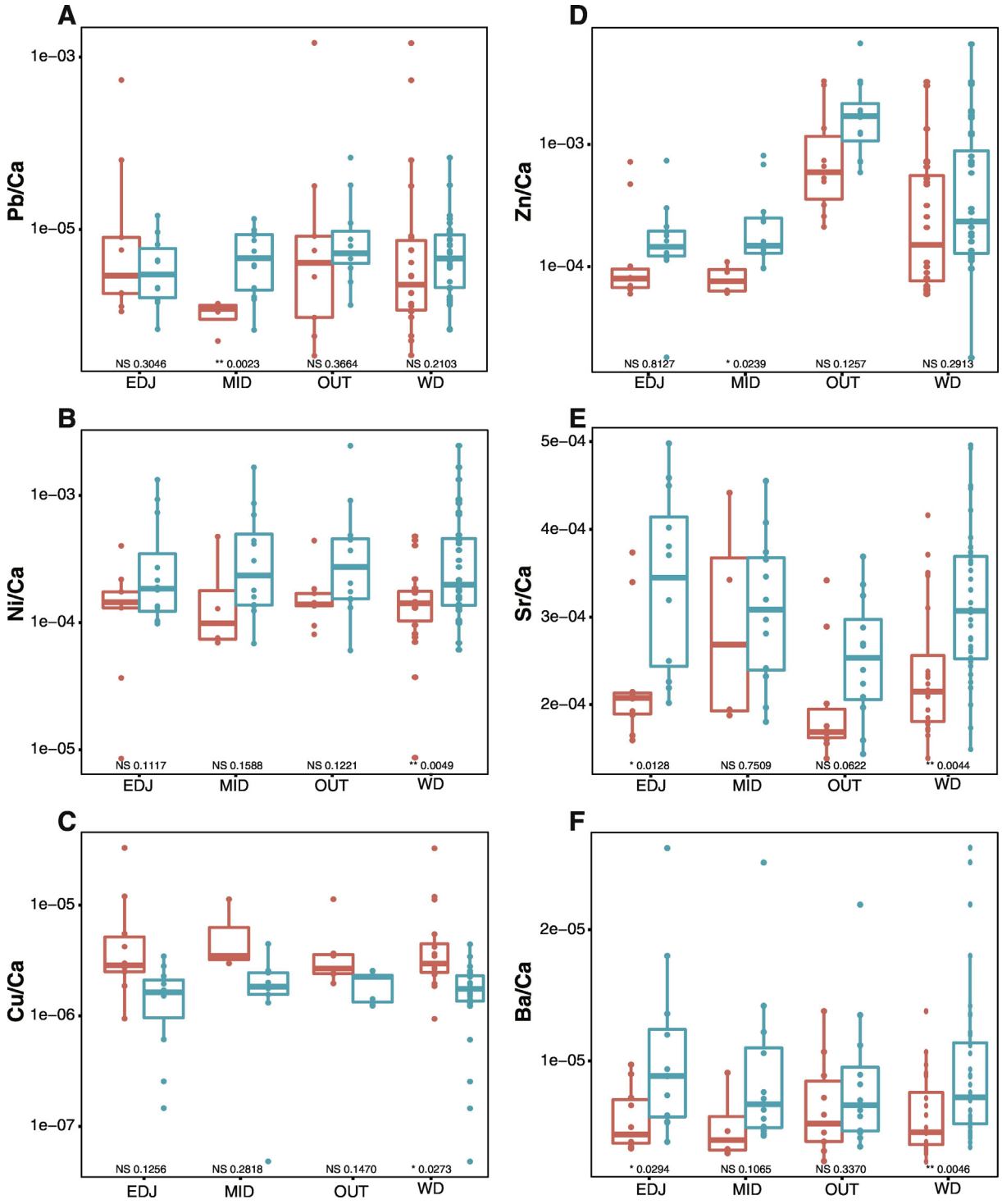

Fig. 2. Distribution of the Ca-normalized ratios in primary (red) and permanent (blue) teeth for the EDJ, MID and OUT profiles and for whole data (WD). Statistical difference between primary and permanent teeth for a given profile and for whole data is estimated using two-tailed Student's *t*-tests *P* values (*P*). For all panels, NS $P > 0.05$, $^{*}P = 0.01$–0.05, $^{**}P = 0.001$–0.01, and $^{***}P < 0.001$. (For interpretation of the references to colour in this figure legend, the reader is referred to the web version of this article.)

Taking the average values of each ratio for all the samples into account, we do not observe any correlation between elements (Table 5).

5. Discussion

5.1. Variations between primary and permanent tooth enamel

All works published so far have compared the elemental composition between pre- and post-natal tooth enamel. Here, we will rather focus on the elemental composition of deciduous and permanent tooth enamel.

Lead is the only element for which the absence of difference between primary and permanent tooth enamel is obvious (Fig. 2A). Regarding the Zn/Ca ratio, the differences between primary and permanent tooth enamel for a given profile are not significant, but this is due to a too low number of analysis (Fig. 2D). Taking the whole data into account does not improve the statistics in the case of Zn, because this mix low Zn/Ca values from "EDJ" and "MID" profiles to high

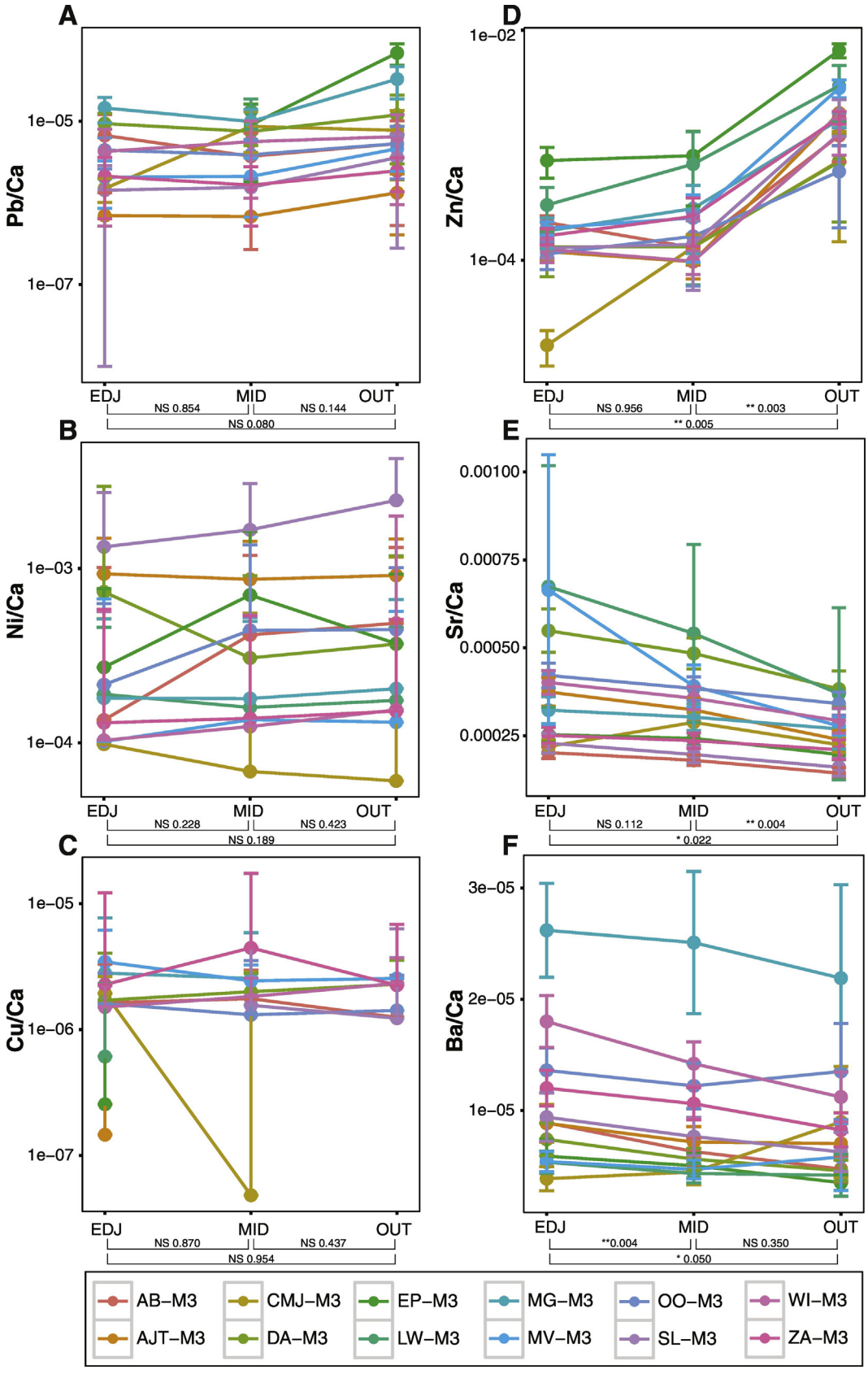

Fig. 3. Distribution of the Ca-normalized ratios in permanent teeth for the EDJ, MID and OUT profiles. Statistical difference between groups of profiles is estimated using two-tailed Student's *t*-tests *P* values (*P*). For all panels, NS $P > 0.05$, $^{*}P = 0.01–0.05$, $^{**}P = 0.001–0.01$, and $^{***}P < 0.001$. Pb/Ca (A), Ni/Ca (B), Cu/Ca (C), Zn/Ca (D) ratios are expressed in log scale, while Sr/Ca (E) and Ba/Ca (F) ratios are expressed in linear scale. (For interpretation of the references to colour in this figure legend, the reader is referred to the web version of this article.)

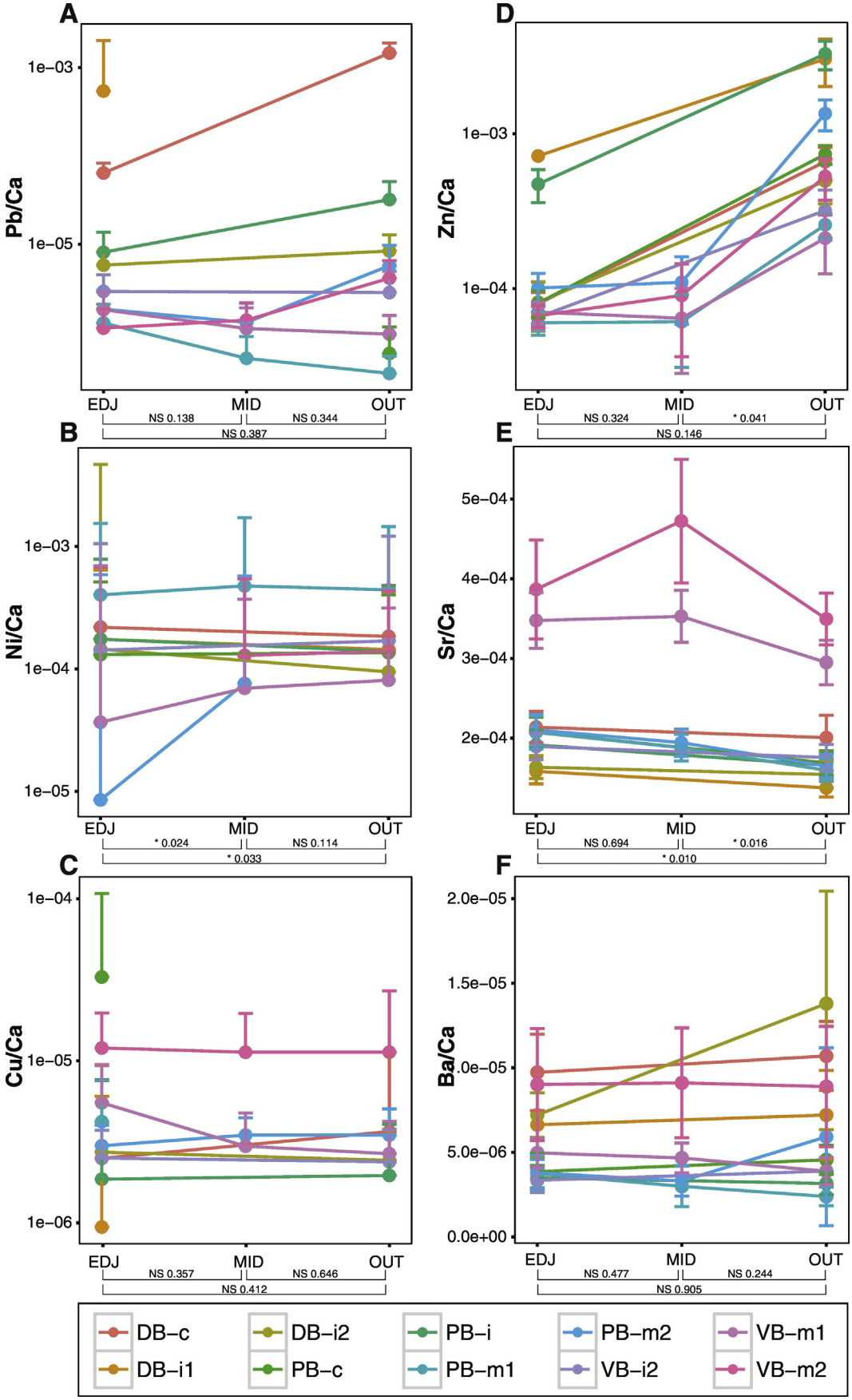

Fig. 4. Distribution of the Ca-normalized ratios in primary teeth for the EDJ, MID and OUT profiles. Statistical difference between groups of profiles is estimated using two-tailed Student's *t*-tests *P* values (*P*). For all panels, NS $P > 0.05$, $^{*}P = 0.01–0.05$, $^{**}P = 0.001–0.01$, and $^{***}P < 0.001$. Pb/Ca (A), Ni/Ca (B), Cu/Ca (C), Zn/Ca (D) ratios are expressed in log scale, while Sr/Ca (E) and Ba/Ca (F) ratios are expressed in linear scale. (For interpretation of the references to colour in this figure legend, the reader is referred to the web version of this article.)

Table 5
Co-variation matrix of the different Ca-normalized ratios.

	Ba/Ca	Pb/Ca	Ni/Ca	Cu/Ca	Zn/Ca	Sr/Ca
Ba/Ca		0.593	0.741	0.590	0.288	0.312
Pb/Ca			0.848	0.605	0.310	0.67
Ni/Ca				0.122	0.723	0.447
Cu/Ca					0.054	0.514
Zn/Ca						0.068
Sr/Ca						

Zn/Ca values from "OUT" profiles (Fig. 2D). The transition metals Ni and Cu exhibit lower and higher Ca normalized ratios, in primary and permanent tooth enamel, respectively. Transition metals are bioessential elements that are metabolically regulated so that, theoretically, no variations of concentration are expected to occur in normal/healthy conditions (Reynard and Balter, 2014). The fact that the Ni/Ca and Cu/Ca ratios vary between primary and permanent tooth enamel suggest that the metabolic regulation of Ni and Cu differ between infancy and adolescence, the two periods of lifetime during which primary and permanent tooth enamels are mineralizing. Another explanation should be that the placenta of the pregnant mother plays a role in the body fluids of her infant, and ultimately in his mineralized tissues, but this would account for pre-natal tooth enamel only. In primary tooth enamel, the alkaline metals Sr and Ba, that share identical electronic properties with Ca, exhibit lower Ca normalized ratios than in permanent tooth enamel. A dietary effect is likely the explanation. Milk Sr/Ca ratio _ with Sr ~20 ng/mL and Ca ~350 μg/mL (Lyengar et al., 1978), leading to a typical Sr/Ca ratio ~6.10^{-6} _ is 500 times lower than that of animal food sources and 1700 times lower than that of plant food sources (Burton et al., 1999; Elias et al., 1982; Gilbert et al., 1994). The milk Ba/Ca ratio equals the Sr/Ca ratio and is 170 times lower than animal food sources and 1170 times lower than plant food sources (Burton et al., 1999; Elias et al., 1982; Gilbert et al., 1994). Therefore milk is very Sr and Ba-depleted relative to other foodstuffs, with an amplitude that corresponds to at least two trophic levels (Balter et al., 2001, 2002). The consumption of milk before weaning can thus explain why the Sr/Ca and Ba/Ca ratios in primary are lower than in permanent tooth enamel.

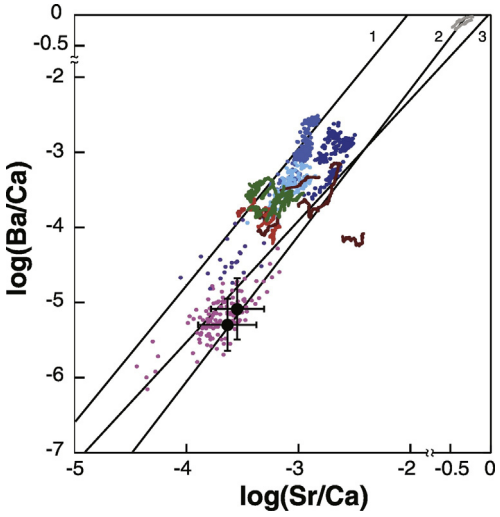

Fig. 6. Compilation of the variations of the Sr/Ca and Ba/Ca ratios in dental enamel obtained using LA-ICPMS. Black circle are for the present study. Pink and purple dots are for humans and monkeys (Austin et al., 2013). Red, green, brown and grey lines are for early *Homo*, *P. robustus*, *A. africanus*, and bovids, respectively (Balter et al., 2012). Light blue, normal blue and dark blue dots, are for wolf, elk and deer, respectively (Kohn et al., 2013). Ca-biopurification regression lines are showed for Burton et al. (1999) (1), Elias et al. (1982) (2) and Gilbert et al. (1994) (3). (For interpretation of the references to colour in this figure legend, the reader is referred to the web version of this article.)

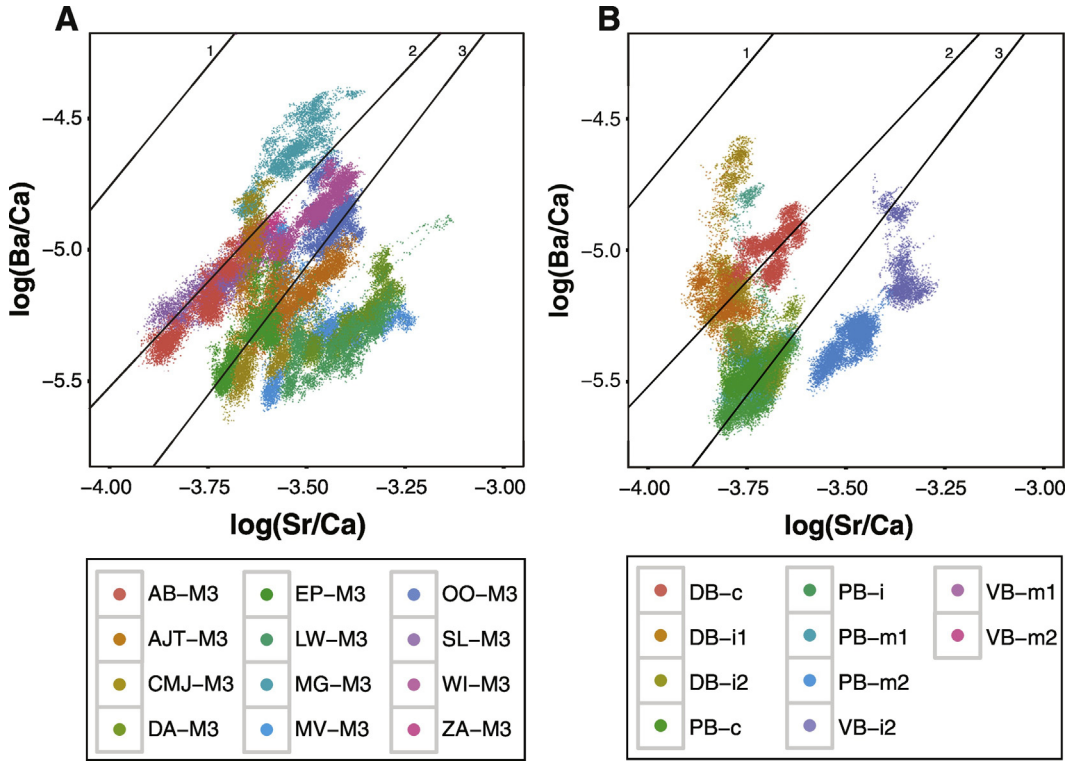

Fig. 5. Variations of the Sr/Ca and Ba/Ca ratios in permanent teeth (A) and primary teeth (B) expressed in log scale. Each point represents a measurement for a total number of ~130,000 measurements. Ca-biopurification regression lines are showed for Burton et al. (1999) (1), Elias et al. (1982) (2) and Gilbert et al. (1994) (3). (For interpretation of the references to colour in this figure legend, the reader is referred to the web version of this article.)

5.2. Variations within primary and permanent tooth enamel

The Pb/Ca, Ni/Ca and Cu/Ca ratios do not vary within tooth enamel, being permanent (Fig. 3A, B, C) or primary (Fig. 4A, B, C). The for the Zn/Ca ratio. The ratio increases in the last few tenth of micron of the outermost part of the enamel, in both permanent and primary tooth enamel (Figs. 3D, 4D, Supplementary Information Maps). Such a pattern has been reported early by Lee et al. (1999), but the increase of Zn was accompanied by concomitant increase of Pb and thus interpreted as a metal contamination. A Zn diffusion through enamel from saliva is unlikely, because most of the third molars were removed while they were still within the bony socket. The pervasive Zn increases in the outermost part of the enamel is more likely due to a biochemical signaling during the mineralization process. Interestingly, it is even conceivable that this biochemical signaling could trigger the termination of teeth formation. The hypothesis has profound implications in the evo-devo field of research but needs further developments.

The present study confirms the results obtained by Humphrey et al. (2008), i.e. there is a decrease of the Sr/Ca ratio from the EDJ region to outer enamel in primary teeth (Fig. 4E), but we extend this observation to permanent teeth (Fig. 3E). Regarding the Ba/Ca ratio, the results are less clear. No significant variation is observed in primary teeth (Fig. 4F), while permanent teeth exhibit an overall significant decrease from the "EDJ" to the "OUT" region (Fig. 3F). Intra-tooth variations of the Ba/Ca ratio were demonstrated to reflect dietary transitions from the introduction of mother's milk through the weaning process in primary teeth (Austin et al., 2013). The pervasive decrease of the Ba/Ca ratio in the permanent teeth suggests that variations in tooth mineralization is also a process at work in the distribution of Ba in tooth enamel, as it is the case for Sr.

5.3. Ca-biopurification in tooth enamel

The process of biological discrimination of Sr and Ba relative to Ca (Ca-biopurification) expresses the positive factor by which Sr and Ba decrease in transferring Ca through physiological reactions (e.g. Wasserman et al., 1957). Elias et al. (1982) demonstrated that Sr/Ca and Ba/Ca decrease in animals with ascending trophic position. This phenomenon was extensively used to reconstruct paleodiet using bone and then enamel which is a more diagenesis-resistant tissue for fossil applications.

At the scale of the trophic chain, the Sr/Ca and Ba/Ca ratios in bone vary linearly when expressed in the log scale, implying that the Ca-biopurification process of Sr and Ba between two subsequent trophic steps are linked by a power law (Balter, 2004). Our results show that the Ca-biopurification process of Sr and Ba in enamel follows the same power law than in bone (Fig. 5A and B). Most of the teeth, being permanent (Fig. 5A) or decidual (Fig. 5B), exhibit a distribution of the Sr/Ca and Ba/Ca ratios that lie along the Ca-biopurification regression lines calculated with bone values. Some of the teeth do seem to escape this rule. This is the case for instance of the VB-m2 tooth, for which there is a decoupling of the Sr/Ca and Ba/Ca ratios, probably due to the cessation of breastfeeding. Such a pattern has already been described for a Neanderthal first molar (Austin et al., 2013).

The fact that the Ca-biopurification process is identical in bone and enamel has two main consequences. The first is that the Sr partitioning coefficients between serum and bone and serum and enamel are similar. This holds for Ba too, and extend the results of Balter and Lécuyer (2010) to the 37 °C temperature. If correct, this implies that bone and enamel can be used equally for paleoenvironmental and paleobiological reconstructions. It is noteworthy that in their survey of Sr/Ca and Ba/Ca

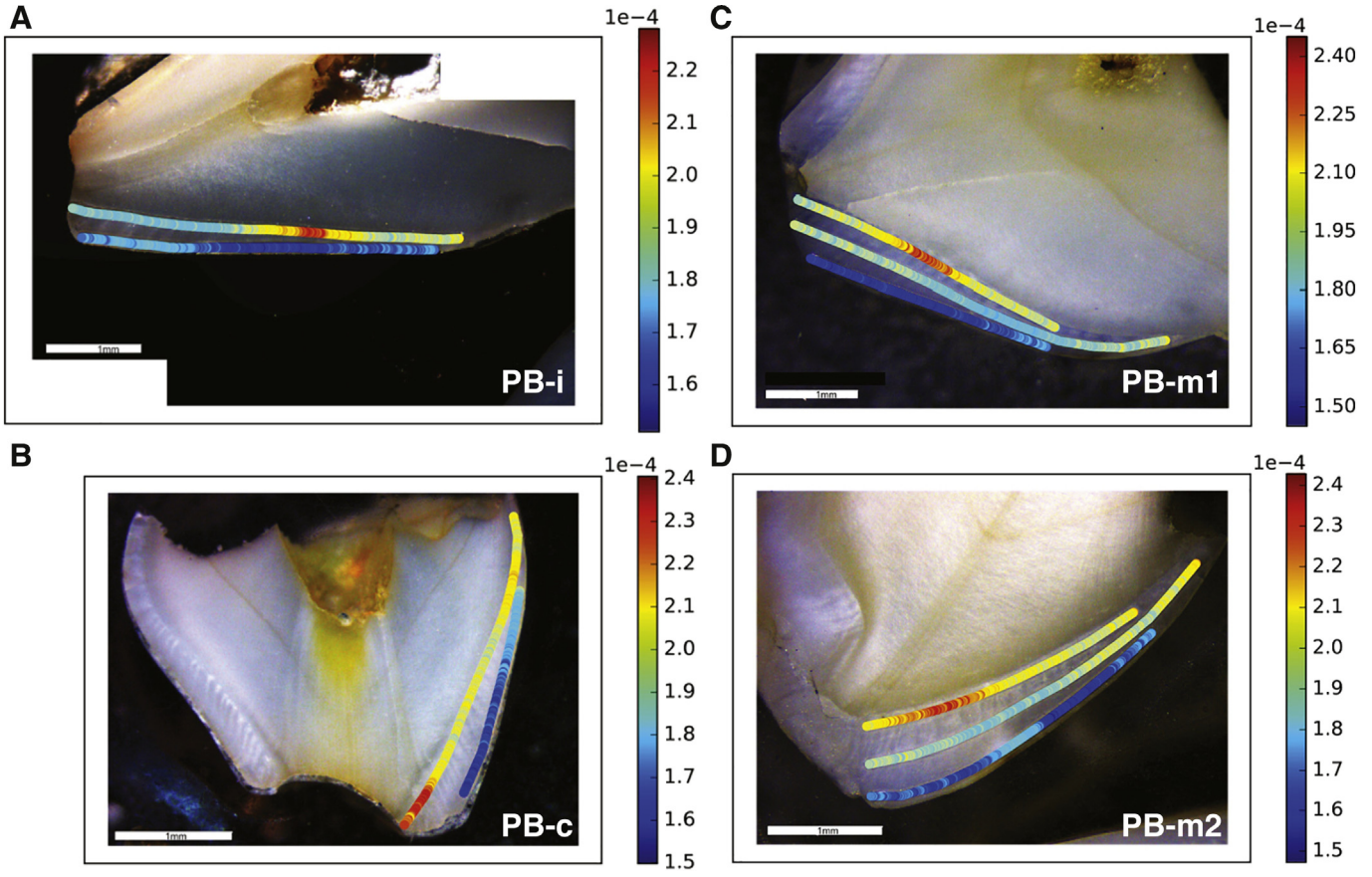

Fig. 7. Maps of the Sr/Ca ratio variation in a primary incisor (A), primary canine (B), primary first molar (C) and primary second molar (D) of the PB individual. (For interpretation of the references to colour in this figure legend, the reader is referred to the web version of this article.)

ratios in dental enamel, Sponheimer and Lee-Thorp (2006) have discovered that grazers and browsers differ in the Sr/Ca and Ba/Ca ratios, however this difference can exist in bone too but have never been tested. The second is that diagenesis could be detected by anomalous departure from the Ca-biopurification area defined by the three existing regression lines. This is perhaps the case for the STS 45 *Australopithecus africanus* sample from the study of Balter et al. (2012) (Fig. 6). However, this sample is characterized by anomalous low Ba concentrations, rather than by anomalous high Sr concentrations, which is hardly compatible with a diagenetic Ba contamination.

5.4. Measurement strategy

Working with computer-assisted laser ablation device allows nowadays to localize precisely the path of the raster on the sample, but the acquisition of a full bio-image is time consuming. Here, we have used two or three paths only. While insufficient to elaborate real bio-images, this was enough to visualize the distribution of the chemical composition of the dental crown of the samples (Supplementary Information Maps). An example is given in Fig. 7. In the example, the Sr/Ca ratios of four primary teeth belonging to the same person are presented. The Sr/Ca excursion seen in the middle of the "EDJ" raster in the incisor (Fig. 7A) is located at the tip of the canine (Fig. 7B) which mineralize soon after the incisor (Al Qahtani et al., 2010). This excursion is also seen in the middle of the "EDJ" raster in the decidual first molar (Fig. 7C) and migrate towards the tip of the crown in the "EDJ" raster of second molar (Fig. 7D). A similar pattern is also observed for the Ba/Ca ratio of these four teeth (Supplementary Information Maps). Therefore it seems that a single event can be located at several places in the dentition with a timeframe compatible with tooth development systematics.

LA-ICPMS can be used also to analyze vast series of tooth samples due to its high throughput capabilities and to the fact that sample chambers are wide enough nowadays to contain several tenth of samples. In such case, it is therefore necessary to evaluate where it is the most interesting area in tooth enamel to process the analysis. Considering that 1) the Zn content can increase by an order of magnitude in the last tenth of microns of outer enamel, and that 2) Sr and Ba are increasingly affected by the degree of mineralization towards outer enamel, we recommend to perform laser ablation raster along the EDJ for a tooth sectioned longitudinally. This strategy of sampling is similar to the one proposed by Zazzo et al. (2005) for carbon isotopes. It holds obviously for tooth samples that can be sectioned. In the other case, i.e. for teeth that cannot be sectioned, naturally broken teeth are the best samples to analyze. In that case, performing rasters from the EDJ areas towards outer enamel along growth prisms, is the best strategy. The number of rasters to performed to maximize the chances to capture any chemical excursion remains to be evaluated with a sampling combining rasters parallel and rasters secant to the EDJ.

6. Conclusions

LA-ICPMS is a powerful technique for the bioimaging of trace elements in tooth enamel, but the information embedded in the complex structure of the enamel is difficult to decipher. Here we use LA-ICPMS to measure Ca-normalized trace elements ratios along profiles from collar enamel to occlusal enamel in 22 primary and permanents teeth. We found some systematic differences between primary and permanent teeth, notably for the Cu/Ca, Ni/Ca, Zn/Ca, Sr/Ca and Ba/Ca ratios, reflecting the *in utero* incorporation of the elements. We also noticed in unworn teeth, being primary or permanent, that Zn content increase dramatically in the last hundred of microns at the enamel surface. This observation is interesting in terms of developmental biology because it can traduce some chemical signals that stop tooth growth. Except for the Zn sharp increase in outer enamel, all the ratios are more or less steady in primary teeth from the EDJ to outer enamel. In contrast, the Sr/Ca and Ba/Ca ratios systematically decrease from the EDJ in permanent teeth. Taking all these observations into account, we propose that one raster along the EDJ will most probably merge all the chemical information.

Supplementary data to this article can be found online at http://dx.doi.org/10.1016/j.scitotenv.2017.06.021.

Acknowledgements

The authors wish to thanks Sergio Ciliberto and Véronique Queste for the financial contribution of the Fonds Recherches of the Ecole Normale Supérieure de Lyon to the laser ablation device. The comments and suggestions of three anonymous reviewers greatly improve the quality of the manuscript. Philippe Dorr is thanked for providing some of the teeth. May all the donors find here the expression of our gratitude to have given us their precious teeth. This work was supported by the project NEXLIZ – CZ.1.07/2.3.00/30.0038.

References

Al Qahtani, S.J., Hector, M.P., Liversidge, H.M., 2010. The London atlas of human tooth development and eruption. Am. J. Phys. Anthropol. 142, 481–490.
Aoba, T., 1996. Recent observations on enamel crystal formation during mammalian amelogenesis. Anat. Rec. 245, 208–218.
Aoba, T., Moreno, E.C., 1990. Changes in the nature and composition of enamel mineral during porcine amelogenesis. Calcif. Tissue Int. 47, 356–364.
Aoba, T., Moreno, E.C., 1992. Changes in the solubility of enamel mineral at various stages of porcine amelogenesis. Calcif. Tissue Int. 47, 356–364.
Arora, M., Kennedy, B.J., Elhlou, S., Pearson, N.J., Walker, D.M., Bayl, P., Chan, S.W.Y., 2006. Spatial distribution of lead in human primary teeth as a biomarker of pre- and neonatal lead exposure. Sci. Total Environ. 371, 55–62.
Arora, M., Hare, D., Austin, C., Smith, D.R., Doble, P., 2011. Spatial distribution of manganese in enamel and coronal dentine of human primary teeth. Sci. Total Environ. 409, 1315–1319.
Asaduzzaman, K., Khandaker, M.U., Baharudin, N.A.B., Bin Mohd Amin, Y., Farook, M.S., Bradley, D.A., Mahmoud, O., 2017. Heavy metals in human teeth dentine: a bio-indicator of metals exposure and environmental pollution. Chemosphere 176, 221–230.
Austin, C., Smith, T.M., Bradman, A., Hinde, K., Joannes-Boyau, R., Bishop, D., Hare, D.J., Doble, P., Eskenazi, B., Arora, M., 2013. Barium distributions in teeth reveal early-life dietary transitions in primates. Nature 498, 216–219.
Balter, V., 2004. Allometric constraints on Sr/Ca and Ba/Ca partitioning in terrestrial trophic chains. Oecologia 139, 83–88.
Balter, V., Lécuyer, C., 2004. Determination of Sr and Ba partitioning coefficients between apatite and water from 5 °C to 60 °C: a new thermometer for aquatic environments. Geochim. Cosmochim. Acta 68, 423–432.
Balter, V., Lécuyer, C., 2010. Determination of Sr and Ba partition coefficients between apatite from fish (*Sparus aurata*) and seawater: the influence of temperature. Geochim. Cosmochim. Acta 74, 3449–3458.
Balter, V., Person, A., Labourdette, N., Drucker, D., Renard, M., Vandermeersch, B., 2001. Were Neandertalians essentially carnivores? Sr and Ba preliminary results of the mammalian palaeobiocoenosis of Saint-Césaire. C. R. Acad. Sci. IIA 332, 59–65.
Balter, V., Bocherens, H., Person, A., Renard, M., Labourdette, N., Vandermeersch, B., 2002. Ecological and physiological variability of Sr/Ca and Ba/Ca in mammals of West European mid-Wurmian foodwebs. Palaeogeogr. Palaeoclimatol. Palaeoecol. 186, 127–143.
Balter, V., Télouk, P., Reynard, B., Braga, J., Thackeray, F., Albarède, F., 2008. Analysis of coupled Sr/Ca and $^{87}Sr/^{86}Sr$ variations in enamel using laser-ablation tandem quadrupole-multicollector ICPMS. Geochim. Cosmochim. Acta 72, 3980–3990.
Balter, V., Braga, J., Télouk, P., Thackeray, F., 2012. Evidence for dietary change but not landscape use in South African early hominins. Nature 489, 558–560.
Budd, P., Montgomery, J., Cox, A., Krause, P., Barreiro, B., Thomas, R.G., 1998. The distribution of lead within ancient and modern human teeth: implications for long-term and historical exposure monitoring. Sci. Total Environ. 220, 121–136.
Budd, P., Montgomery, J., Evans, J., Barreiro, B., 2000. Human tooth enamel as a record of the comparative lead exposure of prehistoric and modern people. Sci. Total Environ. 26, 1–10.
Burton, J.H., Price, T.D., Middleton, W.D., 1999. Correlation of bone Sr/Ca and Ba/Ca due to biological purification of calcium. J. Archaeol. Sci. 26, 609–616.
Copeland, S.R., Sponheimer, M., de Ruiter, D.J., Lee-Thorp, J.A., Codron, D., Le Roux, P.J., Grimes, V., Richards, M.P., 2011. Strontium isotope evidence for landscape use by early hominins. Nature 474, 76–79.
Cox, A., Keenan, F., Cooke, M., Appleton, J., 1996. Trace element profiling of dental tissues using laser ablation-inductively coupled plasma-mass spectrometry. Fresenius J. Anal. Chem. 354, 254–258.
Cucina, A., Dudgeon, J., Neff, H., 2007. Methodological strategy for the analysis of human dental enamel by LA-ICP-MS. J. Archaeol. Sci. 34, 1878–1885.
Dolphin, A.E., Goodman, A.H., Amarasiriwardena, D., 2005. Variation in elemental intensities among teeth and between pre- and postnatal regions of enamel. Am. J. Phys. Anthropol. 128, 878–888.
Eggins, S., Grün, R., Pike, A.W.G., Shelley, M., Taylor, L., 2003. ^{238}U, ^{232}Th profiling and U-series isotope analysis of fossil teeth by laser ablation-ICPMS. Quat. Sci. Rev. 22, 1373–1382.

Elias, R.W., Hirao, Y., Patterson, C.C., 1982. The circumvention of the natural biopurification of calcium along nutrient pathways by atmospheric inputs of industrial lead. Geochim. Cosmochim. Acta 46, 2561–2580.
Evans, R.D., Richner, P., Outridge, M., 1995. Micro-spatial variations of heavy metals in the teeth of walrus as determined by laser ablation ICP-MS: the potential for reconstructing a history of metal exposure. Arch. Environ. Contam. Toxicol. 28, 55–60.
Farell, J., Amarasiriwardena, D., Goodman, A.H., Arriaza, B., 2013. Bioimaging of trace metals in ancient Chilean mummies and contemporary Egyptian teeth by laser ablation-inductively coupled plasma-mass spectrometry (LA-ICP-MS). Microchem. J. 106, 340–346.
Gilbert, C., Sealy, J., Sillen, A., 1994. An investigation of barium, calcium and strontium as palaeodietary indicators in the Southwestern Cape, South Africa. J. Archaeol. Sci. 21, 173–184.
Grün, R., Aubert, M., Joannes-Boyau, R., Moncel, M.-H., 2009. High resolution analysis of uranium and thorium concentration as well as U-series isotope distributions in a Neanderthal tooth from Payre (Ardèche, France) using laser ablation ICP-MS. Geochim. Cosmochim. Acta 72, 5278–5290.
Guede, I., Zuluaga, M.C., Ortega, L.A., Alonso-Olazabal, A., Murelaga, X., Pina, M., Gutierrez, F.J., 2017. Analyses of human dentine and tooth enamel by laser ablation-inductively coupled plasma-mass spectrometry (LA-ICP-MS) to study the diet of medieval Muslim individuals from Tauste (Spain). Microchem. J. 130, 287–294.
Hanć, A., Olszewska, A., Barałkiewicz, D., 2013. Quantitative analysis of elements migration in human teeth with and without filling using LA-ICP-MS. Microchem. J. 110, 61–69.
Hare, D., Austin, C., Doble, P., Arora, M., 2011. Elemental bio-imaging of trace elements in teeth using laser ablation-inductively coupled plasma-mass spectrometry. J. Dent. 39, 397–403.
Hinners, T.A., Hughes, R., Outridge, P.M., Davis, W.J., Simon, K., Woolard, D.R., 1998. Interlaboratory comparison of mass spectrometric methods for lead isotopes and trace elements in NIST SRM 1400 Bone Ash. J. Anal. At. Spectrom. 13, 963–970.
Hinz, E.A., Kohn, M.J., 2010. The effect of tissue structure and soil chemistry on trace element uptake in fossils. Geochim. Cosmochim. Acta 74, 3213–3231.
Hoffmann, E., Stephanowitz, H., Ullrich, E., Skole, J., Lüdke, C., Hoffmann, B., 2000. Investigation of mercury migration in human teeth using spatially resolved analysis by laser ablation-ICP-MS. J. Anal. At. Spectrom. 15, 663–667.
Humphrey, L.T., Dean, M.C., Jeffries, T.E., Penn, T.E.M., 2008. Unlocking evidence of early diet from tooth enamel. Proc. Natl. Acad. Sci. U. S. A. 105, 6834–6839.
Jackson, S.E., Günther, D., 2003. The nature and sources of laser induced isotopic fractionation in laser ablation-multicollector-inductively coupled plasma-mass spectrometry. J. Anal. At. Spectrom. 18, 205–212.
Jaouen, K., Herrscher, E., Balter, V., 2017. Copper and zinc isotope compositions in human bone and enamel. Am. J. Phys. Anthropol. 162:491–500. http://dx.doi.org/10.1002/ajpa.23132.
Kang, D., Amarasiriwardena, D., Goodman, A.H., 2004. Application of laser ablation-inductively coupled plasma-mass spectrometry (LA-ICP-MS) to investigate trace metal spatial distributions in human tooth enamel and dentine growth layers and pulp. Anal. Bioanal. Chem. 378, 1608–1615.
Kohn, M.J., Moses, R.J., 2013. Trace element diffusivities in bone rule out simple diffusive uptake during fossilization but explain in vivo uptake and release. Proc. Natl. Acad. Sci. U. S. A. 110, 419–424.
Kohn, M.J., Morris, J., Olin, P., 2013. Trace element concentrations in teeth – a modern Idaho baseline with implications for archeometry, forensics, and palaeontology. J. Archaeol. Sci. 40, 1689–1699.
Le Roux, P.J., Lee-Thorp, J., Copeland, S.R., Sponheimer, M., de Ruiter, D.J., 2014. Strontium isotope analysis of curved tooth enamel surfaces by laser-ablation multi-collector ICP-MS. Palaeogeogr. Palaeoclimatol. Palaeoecol. 416, 142–149.
Lee, K.M., Appleton, J., Cooke, M., Keenan, F., Sawicka-Kapusta, K., 1999. Use of laser ablation inductively coupled plasma mass spectrometry to provide element versus time profiles in teeth. Anal. Chim. Acta 395, 179–185.
LeGeros, R.Z., LeGeros, J.P., 1984. Phosphate minerals in human tissues. In: Nriagu, J.O., Moore, P.B. (Eds.), Phosphate Minerals. Springer-Verlag, Berlin, pp. 351–385.
Lochner, F., Appleton, J., Keenan, F., Cooke, M., 1999. Multi-element profiling of human deciduous teeth by laser ablation-inductively coupled plasma-mass spectrometry. Anal. Chim. Acta 401, 299–306.
Lugli, F., Cipriani, A., 2017. Commentary on "Analyses of human dentine and tooth enamel by laser ablation-inductively coupled plasma-mass spectrometry (LA-ICP-MS) to study the diet of medieval Muslim individuals from Tauste (Spain)" by Guede et al. 2017. Microchem. J. 130, 287–294 (Microchem. J. 133, 67–69).
Lundgren, T., Persson, L.G., Engstrom, E.U., Chabala, J., Levi-Setti, R., Noren, J.G., 1998. A secondary mass spectroscopic study of the elemental composition pattern in rat incisor dental enamel during different stages of ameloblast differentiation. Arch. Oral Biol. 43, 841–848.
Lyengar, G.V., Kollmer, W.E., Bowen, H.J.M., 1978. The Elemental Composition of Human Tissues and Body Fluids: A Compilation of Values for Adults. Verlag Chemie, Weinheim, New York.
Miliszkiewicz, N., Walas, S., Tobiasz, A., 2015. Current approaches to calibration of LA-ICP-MS analysis. J. Anal. At. Spectrom. 30, 327–338.
Modabbernia, A., Velthorst, E., Gennings, C., De Haan, L., Austin, C., Sutterland, A., Mollon, J., Frangou, S., Wright, R., Arora, M., Reichenberg, A., 2016. Early-life metal exposure and schizophrenia: a proof-of-concept study using novel tooth-matrix biomarkers. Eur. Psychiatr. 36, 1–6.
Outridge, P.M., Veinott, G., Evans, R.D., 1995. Laser ablation ICP-MS analysis of incremental biological structures: archives of trace-element accumulation. Environ. Rev. 3, 160–170.
Pozebon, D., Scheffler, G.L., Dressler, V.L., Nunes, M.A.G., 2014. Review of the applications of laser ablation inductively coupled plasma mass spectrometry (LA-ICP-MS) to the analysis of biological samples. J. Anal. At. Spectrom. 29, 2204–2228.
Reynard, B., Balter, V., 2014. Trace elements and their isotopes in bones and teeth: diet, environments, diagenesis, and dating of archeological and paleontological samples. Palaeogeogr. Palaeoclimatol. Palaeoecol. 416, 4–16.
Shepherd, T.J., Dirks, W., Manmee, C., Hodgson, S., Banks, D.A., Averley, P., Pless-Mulloli, T., 2012. Reconstructing the life-time lead exposure in children using dentine in deciduous teeth. Sci. Total Environ. 425, 214–222.
Shepherd, T.J., Dirks, W., Roberts, N.M.W., Patel, J.G., Hodgson, S., Pless-Mulloli, T., Walton, P., Parrish, R.R., 2016. Tracing fetal and childhood exposure to lead using isotope analysis of deciduous teeth. Environ. Res. 146, 145–153.
Sponheimer, M., Lee-Thorp, J.A., 2006. Enamel diagenesis at South African Australopith sites: implications for paleoecological reconstruction with trace elements. Geochim. Cosmochim. Acta 70, 1644–1654.
Stack, M.V., 1955. The chemical nature of the organic matrix of bone, dentin and enamel. Ann. N. Y. Acad. Sci. 60, 585–595.
Suga, S., 1982. Progressive mineralization pattern of developing enamel during the maturation stage. J. Dent. Res. 61, 1532–1542.
Tacail, T., Télouk, P., Balter, V., 2016. Precise analysis of calcium stable isotope variations in biological apatites using laser ablation MC-ICPMS. J. Anal. Atomic Spectrom. 31, 152–162.
Tacail, T., Thivichon-Prince, B., Martin, J.E., Charles, C., Viriot, L., Balter, V., 2017. Assessing human weaning practices with calcium isotopes in tooth enamel. Proc. Natl. Acad. Sci. U. S. A. http://dx.doi.org/10.1073/pnas.1704412114.
Vašinová Galiová, M., Nývltová Fišáková, M., Kynický, J., Prokeš, L., Neff, H., Mason, A.Z., Gadas, P., Košler, J., Kanický, V., 2013. Elemental mapping in fossil tooth root section of *Ursus arctos* by laser ablation inductively coupled plasma mass spectrometry (LA-ICP-MS). Talanta 105, 235–243.
Wasserman, R.H., Comar, C.L., Papadopoulou, D., 1957. Dietary calcium levels and retention of radiostrontium in the growing rat. Science 126, 1180–1182.
Wilson, P.R., Beynon, A.D., 1989. Mineralization differences between human deciduous and permanent enamel measured by quantitative microradiography. Arch. Oral Biol. 34, 85–88.
Wong, F.S.L., Anderson, P., Fan, H., Davis, G.R., 2004. X-ray microtomographic study of mineral concentration distribution in deciduous enamel. Arch. Oral Biol. 49, 937–944.
Zazzo, A., Balasse, M., Patterson, W.P., 2005. High-resolution $\delta^{13}C$ intratooth profiles in bovine enamel: implications for mineralization pattern and isotopic attenuation. Geochim. Cosmochim. Acta 69, 3631–3642.